NPS63-78-005

NAVAL POSTGRADUATE SCHOOL

Monterey, California

OBSERVATIONS OF THE TEMPERATURE STRUCTURE FUNCTION PARAMETER, C_T^2, OVER THE OCEAN

K. L. Davidson, T. M. Houlihan,
C. W. Fairall, and G. E. Schacher

September 1978

NAVAL POSTGRADUATE SCHOOL
Monterey, California

Rear Admiral T.W. Dedman
Superintendent

J.R. Borsting
Provost

The work reported herein was supported in part by the Naval Ocean Systems Center (EOMET).

This report was prepared by:

G. Haltiner, Chairman
Department of Meteorology

William M. Tolles
Dean of Research

UNCLASSIFIED

SECURITY CLASSIFICATION OF THIS PAGE (When Data Entered)

REPORT DOCUMENTATION PAGE

READ INSTRUCTIONS BEFORE COMPLETING FORM

1. REPORT NUMBER: NPS-63Ds78005	2. GOVT ACCESSION NO.
3. RECIPIENT'S CATALOG NUMBER	
4. TITLE (and Subtitle): OBSERVATIONS OF THE TEMPERATURE STRUCTURE FUNCTION PARAMETER, C_T^2, OVER THE OCEAN	5. TYPE OF REPORT & PERIOD COVERED: Oct 1977 - Oct 1978
	6. PERFORMING ORG. REPORT NUMBER
7. AUTHOR(s): K. L. Davidson, T. M. Houlihan, C. W. Fairall, and G. E. Schacher	8. CONTRACT OR GRANT NUMBER(s): N00019-78-WR-81002; N66001-78-WR-00156
9. PERFORMING ORGANIZATION NAME AND ADDRESS: Naval Postgraduate School, Monterey, CA 93940	10. PROGRAM ELEMENT, PROJECT, TASK AREA & WORK UNIT NUMBERS
11. CONTROLLING OFFICE NAME AND ADDRESS: Naval Oceans Systems Center, San Diego, CA 92152	12. REPORT DATE: September 1978
	13. NUMBER OF PAGES: 45
14. MONITORING AGENCY NAME & ADDRESS (if different from Controlling Office)	15. SECURITY CLASS. (of this report): UNCLASSIFIED
	15a. DECLASSIFICATION/DOWNGRADING SCHEDULE

16. DISTRIBUTION STATEMENT (of this Report)

Approved for public release; distribution unlimited. Reproduction in whole or in part is permitted for any purpose of the United States Government.

17. DISTRIBUTION STATEMENT (of the abstract entered in Block 20, if different from Report)

18. SUPPLEMENTARY NOTES

19. KEY WORDS (Continue on reverse side if necessary and identify by block number)

Temperature structure, Boundary layer, Turbulence

20. ABSTRACT (Continue on reverse side if necessary and identify by block number)

Observational results from shipboard measurements of temperature fluctuations, and mean wind, temperature, and humidity, are compared with existing expressions for the surface flux and height dependence of C_T^2. Surface flux estimates are obtained from bulk aerodynamic formulae. Temperature fluctuation data are selected to minimize a salt-contamination effect which causes increases in temperature variance. Predictions for C_T^2 based on surface flux scaling agree within 20%, except for near neutral and large

DD FORM 1 JAN 73 1473 EDITION OF 1 NOV 65 IS OBSOLETE S/N 0102-014-6601 |

UNCLASSIFIED

SECURITY CLASSIFICATION OF THIS PAGE (When Data Entered)

unstable conditions where the disagreement can be attributed to measurement problems.

Table of Contents

Observations of the temperature structure function parameter, C_T^2, over the ocean

K. L. Davidson, T. M. Houlihan, C. W. Fairall and G. E. Schacher

Environmental Physics Group
Naval Postgraduate School
Monterey, CA 93940

Abstract

Observational results from shipboard measurements of temperature fluctuations, and mean wind, temperature, and humidity, are compared with existing expression for the surface flux and height dependence of C_T^2. Surface flux estimates are obtained from bulk aerodynamic formula. Temperature fluctuation data are selected to minimize a salt-contamination effect which causes increases in temperature variance. Predictions for C_T^2 based on surface flux scaling agree within 20%, except for near neutral and large unstable conditions where the disagreement can be attributed to measurement problems.

1. Introduction

The atmospheric marine surface layer is that region in the first 50 meters or so over the sea which is characterized by large turbulent vertical transfer of momentum, heat, and moisture. Progress has been made in specifications of surface wind fields and hydrostatic stability for this region since these are parameters used in estimating boundary fluxes in numerical atmospheric prediction and for predicting changes in the upper part of the ocean. Another interest in this region is the quantification of turbulent effects on optical wave propagation. The optical effects occur at scales which are smaller than those associated with boundary fluxes. This involves specifications of fluctuations in velocity, temperature, and humidity for scales approaching those responsible for viscous dissipation of turbulent kinetic energy and molecular diffusion of scalar (temperature and humidity) quantities.

Existing measurement capabilities and turbulence theory enable observations of the small scale properties of interest, but the complexities and cost of such direct observations inhibit them on routine bases. Therefore, there is a need to examine relationships between the small scale properties and the more feasibly measured parameters: the mean winds, temperature, and humidity.

Descriptions of the small scale turbulent properties have not been as complete nor in the quantity for the overwater regime as for the overland regime (described by Champagne, et al., 1977). The overwater regime requires separate considera-

tion because of evidence of influence on the airflow by the surface waves (Davidson, 1974) and the importance of the water vapor content of the air. The water vapor effects are manifested both in atmospheric stability and in optical propagation.

For optical waves, the largest contributors to the refractive-index fluctuations are temperature fluctuations (T'). Friehe, et al. (1975) have shown that another significant contributor may be the temperature-humidity fluctuation covariance. They observed a contribution of 24% to the refractive index structure function parameter, C_n^2, from humidity effects during a time when the temperature-humidity covariance was positive.

The intensity of temperature fluctuations for scales from a few millimeters to several meters can be characterized by the temperature structure function parameter, C_T^2, defined as

$$C_T^2 = \frac{D_T(r)}{r^{2/3}} \qquad (1)$$

$D_T(r)$ is defined as $D_T(r) = \overline{[T(x) - T(x+r)]^2}$ where T(x) and T(x+r) are temperature at two points on a line oriented normal to the mean wind direction separated by the distance r.

The temperature structure function parameter can also be related to small scale processes of turbulent kinetic energy dissipation and heat diffusion by the following expression

$$C_T^2 = \eta\, \varepsilon^{-1/3}\, \chi \qquad (2)$$

where η is a constant equal to 3.2, ε is the dissipation rate of turbulent kinetic energy and χ is the rate at which the temperature inhomogeneities are diffused or "smeared" out. Equation 2 arises from two parallel expressions for the one-dimensional variance spectrum for temperature fluctuations in the inertial subrange.

$$S_T(k) = \alpha\ C_T^2\ k^{-5/3} \tag{3}$$

and

$$S_T(k) = \beta\ \varepsilon^{-1/3}\ \chi\ k^{-5/3} \tag{4}$$

where α and β are constants equal to .25 and .8 respectively. The latter expression was formulated by Corrsin (1951).

This paper describes results from a comparison of a very substantial amount of C_T^2 data obtained over the open ocean with the Wyngaard et al. (1971) predictions based on bulk surface layer measurements. Friehe (1976) performed a similar comparison in which fewer data were used and in which a different bulk stability parameter was used. He concluded that reasonable prediction of C_T^2 could be made from bulk formulations.

2. Surface Layer Bulk Aerodynamic Relations for C_T^2

Wyngaard, et al. (1971) related C_T^2 to surface fluxes with Eq. 2 using separate expressions for ε and χ based on overland measurements. The general expression was

$$\frac{C_T^2\ Z^{2/3}}{T_*^2} = f(\xi);\ \xi = \frac{Z}{L} \tag{5a}$$

where $f(\xi) = \begin{cases} 4.9(1 - 7\xi)^{-2/3} & \xi < 0 \quad (5b) \\ 4.9(1 + 2.4\,\xi^{2/3}) & \xi > 0 \quad (5c) \end{cases}$

It is noted that these interpolation formulae still lack substantial verification for the overwater regime.

These formulae agree with the expected asymptotic scaling (Wyngaard, 1973) for C_T^2 under very unstable (local free convection) and very stable (Z-less) stratifications. The appropriate scaling formulations in the extreme stability limits are

$$\text{free convection:} \quad \frac{C_T^2 \, Z^{2/3}}{T_f^2} = \text{constant} \qquad (6)$$

where $T_f = (TQ_o^2/gZ)^{1/3}$; $Q_o = \overline{w'\theta'}$

$$\text{Z-less:} \quad \frac{C_T^2 \, L^{2/3}}{T_*^2} = \text{constant} \qquad (7)$$

Therefore, the asymptotic predictions are for C_T^2 to vary as $Z^{-4/3}$ for free convection and to be independent of height (Z-less) for very stable conditions.

In this study, boundary flux parameters in Eq. 5 , (T_* and L) were calculated using bulk aerodynamic formulae. Bulk aerodynamic formulae are those which relate boundary scaling parameters to the wind speed at a level and the temperature and humidity difference between that level and the surface. Their use for indirect estimates of the boundary fluxes has received considerable attention in overwater observational experiments because of difficulties in making eddy flux, and profile measurements.

The bulk aerodynamic formulae at a height Z for the velocity and potential temperature scaling parameters are:

$$u_* = C_D^{\frac{1}{2}} U \tag{8}$$

$$T_* = C_\Theta^{\frac{1}{2}} (\Theta_Z - \Theta_S) \tag{9}$$

where S refers to the surface value and C_D and C_Θ are drag coefficients. The drag coefficients depend upon height, stability, and wind velocity. Similarly, for the sensible heat flux

$$-\overline{w'\Theta'} = C_H U (\Theta_Z - \Theta_S) \tag{10}$$

where

$$C_H = (C_D C_\Theta)^{\frac{1}{2}} \tag{11}$$

Since several publications give detailed descriptions of the bulk method with various experimental values for the drag coefficients, we shall restrict this discussion to a few points that must be considered when relating overwater measured values of C_T^2 to values of T_* and ξ based on bulk method calculations. In particular, we must note that T_* is directly dependent upon the value of $C_\Theta^{\frac{1}{2}}$ (Eq. 9). Using conventions developed by Liu (1978), the neutral stability temperature drag coefficient is given by (in this convention, $(\alpha_T \kappa Z/T_*)(\partial\theta/\partial Z)$ is the dimensionless profile function)

$$C_{\Theta N}^{\frac{1}{2}} = \alpha_T \kappa [\ell n(Z/Z_{oT})]^{-1} \tag{12}$$

where κ is von Karman's constant, α_T the ratio of heat and momentum transport diffusivities (at neutral stability) and Z_{oT} is the appropriate roughness length for the temperature profile. Since Wyngaard, et al.'s expression for $f(\xi)$ was based upon direct measurement of T_* from the heat flux and Reynold's stress, their curve was not dependent upon a choice of $C_{\theta N}$. In view of this, we will select the value of $C_{\theta N}$ that yields the best fit to our data, treating this as an indirect measurement of $C_{\theta N}$.

The dependence of overwater neutral momentum drag coefficients, C_{DN}, on wind speed has been the objective of many investigations. For our analyses, we chose a recently suggested representation by Kondo (1975), Table 1.

The stability dependence of C_D and C_θ is defined on the basis of the following general expressions

$$C_D = \frac{C_{DN}}{[1 - (\kappa)^{-1} C_{DN}^{\frac{1}{2}} \psi_1(\xi)]^2} \tag{13}$$

$$C_\theta = \frac{C_{\theta N}}{[1 - (\alpha_T \kappa)^{-1} C_{\theta N}^{\frac{1}{2}} \psi_2(\xi)]^2} \tag{14}$$

where $\psi_1(\xi)$ and $\psi_2(\xi)$ are stability corrections to wind and scalar profiles. Formulations for $\psi_1(\xi)$ and $\psi_2(\xi)$ have been presented by Businger (1973) and ours were similar except for the use of α_T normalization (Liu, 1978).

The dependence of the drag coefficients on stability leads to computational considerations in estimating ξ since the coefficients which define the latter are themselves functions

of ξ as indicated by the following bulk expression

$$\xi = \xi_o \left[\frac{(1 - \kappa^{-1} C_{DN}^{\frac{1}{2}} \psi_1(\xi))^2}{(1 - (\alpha_T \kappa)^{-1} C_{\theta N}^{\frac{1}{2}} \psi_2(\xi)} \right] \quad (15)$$

where

$$\xi_o = \kappa \frac{gZ}{T} \frac{C_{\theta N}^{\frac{1}{2}}}{C_{DN}} \left[\frac{\Delta\theta + .18\Delta Q}{U^2} \right] \quad (16)$$

All parameters are in the MKS units with Q in gm/kg. ξ_o is the equivalent of a first guess of ξ based on bulk differences and neutral values for the drag coefficients. For each value of wind velocity, we calculated C_{DN}, allowing calculation of ξ_o. The final value of ξ was found by solving Eq. 15, iteratively. An example set of solutions is shown in Fig. 1 for U = 7.6 m/sec.

Friehe (1976) effectively defined ξ as being equal to ξ_o when he compared overwater C_T^2 values with bulk parameter predictions based on Eq. 5. He used a constant C_{DN} value and two different values of $C_{\theta N}$, depending on the value of $U\Delta\theta$. The differences between the solid curve and dashed lines in Fig. 1 represent the difference which would arise in neglecting stability effects in the specification of ξ.

3. Experimental Arrangements

The data were obtained during several experiments conducted during a four year period (1974-1978), over an extensive ocean area and aboard three different ships (listed in Table 2). The instrumentation was designed for profile measurements of both mean and turbulent parameters. In all experiments, these were made at multi-levels on two masts separated spatially on the

forward part of the ships (Fig. 2). A comprehensive description of the system is the subject of another paper (Houlihan, et al., 1978).

Mean temperature was measured with quartz oscillator thermometers, accurate to .01°C. Mean humidity was measured with Li Cl sensors, accurate to about 3%RH. Wind velocity was measured with cup anemometers, accurate to about 5%. Temperature fluctuations (for C_T^2) were measured with ac Wheatstone bridges (3.0 KHz carrier), using paired resistance probes with 2.5μm diameter platinum wires. The resistance probes were mounted on wind vanes to maintain correct alignment with the relative wind direction.

Two features of the measurement arrangement significant in the interpretation of results are the aspiration of mean temperature sensors and the surface temperature measurements. The quartz temperature sensors and humidity sensors were contained within aspirated weather shelters. The shelters had two purposes: to protect the sensors from the marine environment and to reduce radiation effects. Radiation effects were of special concern, since some of the sensors were above the water and some were above the deck of the ships, which are heated by the sun and radiate strongly. Because of radiation from the deck, we modified the shelters, placing a shield at the base of the unit to reduce radiation from below. Even with these precautions, systematic temperature corrections for the aspirators (during day and night operations) have been determined from calibrations with a glass dewar type aspirator. The daytime correction .6C and the nighttime correction is .4C (subtracted from measured temperature).

The sea surface temperature sensor (a quartz probe) was attached to a plastic hose so that it floated within one inch of the surface. On all ships, its location was aft of the midship. The location on all of these ships, underway and holding position, was definitely influenced by the ship's wake.

The mean data were continuously averaged and periodically logged by a microprocessor developed at the Naval Postgraduate School and adopted for the R/V ACANIA by Plunkett (1977). Mean values were defined for 15 to 30 minute periods. Most periods were 30 minutes long, the planned duration, but shorter periods occurred due to such events as change in the ship's course.

4. Data Evaluation and Error Analysis

Comparison of C_T^2 results and available expressions are made with T_* and L values estimated from 10 meter wind, temperature, and humidity and surface temperature values. Initial plans were also to estimate T_* and L values from mean profile data, as evident from previously described instrumentation arrangements. The latter results are not presented because of inconsistencies which have been attributed to difficulties in defining small scalar and wind gradients. Although these same errors existed in the mean data used for bulk estimates, the accuracy requirements of the bulk method are much less stringent.

The 10 meter mean, as well as C_T^2 values, were obtained by interpolating from levels above and below, if available, or by extrapolating on the basis of expected height variations, if only one level was available. With these specifications, T_* and ξ were computed for the 10 meter level, using Eqs. 9 and 15.

Two aspects of the measurements require further discussion for this study. These are the influence of salt contamination on resistance wire sensors, and uncertainties in the surface temperature specification. Although the latter may not be significant for some applications, it is significant in our results, because the air-surface temperature difference occurs as a squared quantity in scaling C_T^2 by T_*^2.

The influence of salt contamination of resistance wires and thermocouples, and hence, all temperature fluctuation measurements in the marine environment, was recently described by Schmitt, et al. (1978). These effects were discussed by Friehe (1977) in his comparison between overwater C_T^2 values and bulk aerodynamic predictions and led him to limit the data considered. Schmitt, et al. (1978) suggested that erroneous temperature fluctuations occur due to water vapor absorption and evaporation on the salt nuclei attached to the wire. This occurs in conjunction with fluctuations in ambient RH. The effect is manifested by the occurrence of spikes in the temperature trace. These spikes can cause overwater temperature variance spectra to exhibit non-Kolmogorov slopes.

In an effort to eliminate the salt effect, the resistance wires were washed or changed at frequent intervals during the latest experiment (CEWCOM-78). Mean ratios of C_T^2 immediately before and after washing versus relative humidity appear in Fig. 3. We observed that C_T^2 values from contaminated wires are larger for an RH range from 50% to 85%, only. Presumably, the effect is diminished at RH above 85% because humidity fluctuations are less intense due to the small RH gradient. Their effect, as described, is within the system accuracy. Presumably, the effect is diminished at RH below 50% because the salt nuclei attached to the wires are not activated, hence, humidity fluctuations do not cause significant absorption or evaporation.

We tested these interpretations by computing the ratio of measured C_T^2 to computed C_T^2 (using Eq. 5 and bulk parameter estimates of T_* and ξ) with data from all experiments except CEWCOM-78. Mean values of these ratios versus RH appear in Fig. 4. The individual points are mean values for 5% RH intervals and the error bars are expected errors of the averages ($\pm \sigma/\sqrt{N}$, N = number of points) within each interval. The number at the top of the error bar is N. These data exhibit values near 1 for RH values above 85%. There are slight increases at 95% and at 85% and there is a significant increase at 80%. The ratios are larger at low RH values, compared to corresponding result from clean wires in CEWCOM-78.

Differences between the results in Fig. 3 (washing and replacement) and the results in Fig. 4 (from the other experiments) are the larger values of the ratio at very low RH values and the

lower values above 95%. The former result is not unexpected, because wires exposed for longer periods without cleaning as they were for the other experiments would be sufficiently contaminated to respond to large humidity fluctuations, even if they were not activated. The latter result could also be attributed to the degree of contamination and the tendency of salt particles to grow into water droplets at high RH. Contaminated wires at large RH values experience a loss of frequency response, resulting in a lower sensitivity to temperature fluctuations.

Based on the above results, we decided to consider only those C_T^2 data measured at RH values above 82.5%. C_T^2 results obtained with lower RH values were excluded except from periods immediately following sensor replacement. All data from CEWCOM-78 which were from clean sensors were considered.

We used intermediate C_T^2 and $\Delta\theta$ results to examine uncertainties in the sea surface temperature. These results appear in Fig. 5 where C_T^2 data were selected on the basis of RH considerations and $\Delta\theta$ values have been adjusted for systematic aspirator corrections. If the measured surface temperatures were the "skin" temperatures, we expect the minimum in C_T^2 to occur near $\Delta\theta$ equal to zero. This is the case for both night and day. However, we estimate that our $\Delta\theta$ values are subject to uncertainties as large as $.5^{\circ}C$, based on the displacement and broadness of the daytime C_T^2 minimum. This is primarily due to an inability to ensure that the sea surface sensor actually measured the skin temperature. Liu (1978)

suggests how the latter problem could have been treated with interface flux equilibrium considerations. However, his suggested procedures were not applied to these data because they apply to a bucket temperature which was not measured by our sensor.

The results of an analysis of measurement errors appear in Table 3. These are the errors introduced by instrument acccuracies, noise and uncertainties in certain calibration values. In the case of C_T^2, most of the uncertainty is due to the salt contamination effect. In the case of T_S, the sensor itself is accurate to .01°C, but one cannot be certain that the sensor is in fact measuring the surface temperature.

5. Results

Dimensionless temperature structure parameter (DTSP) versus ξ results appear in Fig. 6, in the format used by Wyngaard, et al. (1971). Again, error bars are the uncertainties of the means and the numbers are the number of points defining the mean. For this comparison, $C_{\theta N}$ was determined by assuming that Z_{oT} was independent of velocity and had a value corresponding to Z_o for a typical drag coefficient, $C_{DN} = 1.3 \times 10^{-3}$. The appropriate value of $C_{\theta N}$ for a measured C_T^2 was estimated from the following equation,

$$C_{\theta N} = \left(\frac{C_T^2 \, Z^{2/3}}{f(\xi)}\right) \frac{\left[1 - (\ell n \, Z/Z_{oT})^{-1} \, \psi_2(\xi)\right]^2}{\Delta\theta^2} \qquad (17)$$

The value of $C_{\theta N}$ selected was that from the CEWCOM-78 data, since these were least influenced by salt contamination.

Although it was necessary to assume an initial value of $C_{\theta N}$ to obtain the values of ξ, the final results (Fig. 7)

are fairly insensitive to the initial choice. A minimum $|\xi|$ value of .05 was used in this determination in view of the uncertainties listed in Table 3. The value of $C_{\theta N}$ selected and, hence, used to compute T_* and ξ for the results in Fig. 6 was 1.3×10^{-3}. Using $C_{HN} = (C_{DN}\, C_{\theta N})^{\frac{1}{2}}$, we compare this $C_{\theta N}$ value with some obtained from measurements of C_{HN} (Table 4), assuming a typical C_{DN} value of 1.3×10^{-3} if not given.

DTSP results are also presented with logarithmic ξ axes, Fig. 8. This format enables examination of the distributions of the large number of results near ξ equal to zero in a more illustrative perspective. Also, results at ξ values less than -7 which were not included in Fig. 6, can now be viewed.

This format demonstrates the exceptional agreement between the results and the prediction over the range, $-.03 < \xi < -7$. Also, disagreement between observed and predicted results can be readily related to previously mentioned measurement uncertainties. Disagreements at the minimum $|\xi|$ intervals, for both stable and unstable sides, are attributed to errors in specifying $\Delta\theta$ as well as inherent noise in the C_T^2 measurement and recording systems. Disagreement at large $|\xi|$ values on the unstable side is attributed to increased C_T^2 values due to the salt contamination effect, since these data happen to have corresponding relative humidity values near 85%.

DTSP results based on asymptotic scaling for unstable (Eq. 6, free convection) and stable (Eq. 7, Z-less) conditions appear in Figs. 9a and 9b, respectively. Predictions based on

Eq. 5 (a and b) appear as solid curves. For the unstable side, the prediction was approximated as

$$\frac{C_T^2 \, Z^{2/3}}{T_f^2} = 9.9 \quad \frac{|\xi|}{1-7\xi}^{2/3} \tag{18}$$

which approaches a value of 2.7 for large $|\xi|$. Eq. 18 is not correct when q_*, as well as T_*, determines ξ. When q_* is negative (typical marine conditions), the observed values should be less than predicted by this expression. This is the case for these results. For the stable side, the prediction is

$$\frac{C_T^2 \, L^{2/3}}{T_*^2} = 4.9 \, [\xi^{-2/3} + 2.4] \tag{19}$$

which approaches a value of 11.8 for large ξ.

In summary, the DTSP results agree very well with the predictions under unstable conditions and reasonably well under stable conditions. Under stable conditions, they are slightly less than the predictions. The determined $C_{\theta N}$ value agrees reasonably well with those reported. DTSP disagreement under neutral conditions ($|\xi| < .05$) is attributed to uncertainties in measuring the air-sea temperature difference and inherent system and measurement noise. The latter would include the salt contamination effect, since any humidity fluctuation would cause apparent temperature fluctuations. Disagreement under very unstable conditions, $\xi < -7$, was due to the fact that these data occurred with

RH values, $\tilde{=}$ 85% , not totally immune to the salt contamination effect.

The actual significance of the slight disagreement under stable conditions is somewhat uncertain. However, it could also be attributed to the salt contamination effect. During stable conditions over the ocean, humidity and temperature fluctuations are negatively correlated. Hence, dry-warm or moist-cold eddies are causing the fluctuations. In the case of dry-warm parcels, contaminated sensors would be experiencing a cooling due to evaporation, but a compensating heating due to the temperature change would also occur. In the case of cold-moist parcels, the reverse would occur.

DTSP results based on asymptotic scaling appeared to approach the predicted constants at the limits. Agreement for these results was expected, on the basis of agreement in other DTSP results, because Monin-Obukhov scaling was used in determining T_f. This arose when Q_o, in Eq. 6, was determined from T_* and U_* values which were estimated on the basis of Monin-Obukhov scaling.

The multi-level C_T^2 data enabled an examination of predicted height variation, under different stability conditions. These results appear in Fig. 10 where A is the coefficient obtained for the best fit linear relation between observed Log C_T^2 values and Log Z values,

$$\text{Log } C_T^2 = A \text{ Log } Z + B. \qquad (20)$$

The curves are predictions obtained by determining dLog C_T^2/dLog Z from Eq. 5 and approach limiting values of -4/3 and 0 on the unstable and stable sides and a value of -2/3 at the neutral point.

Fewer periods were available for this examination than for the preceding C_T^2 results. This was because probes at upper levels, which were not readily accessible, were not always replaced when they became inoperative. Also, we measured C_T^2 at a single level during CEWCOM-78 because of frequent probe washing and replacement.

Results in Fig. 10 indicate that height dependence of observed C_T^2 values agreed quite well with the prediction. This is particularly the case for the stability variation of the dependence. A majority of the mean values indicate that C_T^2 decreased somewhat less rapidly with height than the prediction. This result could be attributed to system noise which contributed the same at all levels and would reduce the apparent relative difference (decrease) between levels. Evidence for this is the larger (relative) disagreement at near neutral (unstable) intervals, where the signal to noise ratio is the smallest.

6. Conclusions

Comparisons of a substantial amount of overwater C_T^2 data have been made with predictions of the existing empirical expressions. Measured overwater C_T^2 data, which were selected to minimize the salt contamination influence are described

very well by Wyngaard, et al's (1971) expressions, even with bulk surface flux estimates. An estimated $C_{\theta N}$ valu of 1.3×10^{-3} agrees with lower values obtained by others. Disagreements exceeding measurement accuracies (20-30%) occur for near neutral conditions where C_T^2 is insignificant in most applications, and for large unstable conditions. These disagreements are attributed to measurement difficulties rather than to the validity of the existing expressions. Agreement between observed and predicted height distributions over the full stability range provide further verification of the existing expression.

In conclusion, a typical (but not the best) comparison of observed and predicted C_T^2 values during a 24 hour period in CEWCOM-78 is presented in Fig. 11a to further demonstrate the overwater applicability of the expressions. The predicted values based on bulk estimates of surface fluxes are within the accuracy of the measurements in describing the observed values. Coincident bulk $|\xi|$ estimates for the period appear in Fig. 11b.

ACKNOWLEDGEMENTS

Work supported by the following commands of the U. S. Navy: Oceanographer of the Navy (Code 3100), Naval Sea Systems Command (PMS 405), and Naval Air Systems Command (AIR 370).

We wish to acknowledge the contributions of Ray Garcia, Lyn May, Steven Rinard, Jeffrey Haltiner, Charles Leonard, Vicki Culley, and Captain Reynolds and the crew of the R/V ACANIA.

REFERENCES

Businger, J. A. (1973): "Turbulent Transfer in the Atmospheric Surface Layer," Chapter 2, Workshop on Micrometeorology, D. Harugen, Editor, American Meteorological Society, 67-98.

Champagne, F. H., Friehe, C. A., LaRue, J. C., and Wyngaard, J. C., (1977): "Flux Measurements, Flux Estimation Techniques and Fine-Scale Turbulence Measurements in the Unstable Surface Layer Over Land." J. Atmos. Sci., 34. 513-530.

Corrsin, S. (1951): "On the Spectrum of Isotropic Temperature Fluctuations in an Isotropic Turbulence," J. Appl. Phys., 22, 469-473.

Davidson, K. L. (1974): "Observational Results on the Influence of Stability and Wind-Wave Coupling on Momentum Transfer and Turbulent Fluctuations over Ocean Waves, Boundary Layer Meteorology, 6, 305-331.

Dunckel, M., Hasse, L., Krugermeyer, L., Schriever, D., and Wucknitz, J., (1974): "Turbulent Fluxes of Momentum, Heat and Water Vapor in the Atmosphere Surface Layer at Sea During ATEX, Boundary Layer Meteorl., 6, 81-106.

Friehe, C. A. (1976): "Estimation of the Refractive-Index Temperature Structure Parameter in the Atmospheric Boundary Layer over the Ocean," Applied Optics, 16, 334-340.

Friehe, C. A., LaRue, J. C., Champagne, F. H., Gibson, C. H., and Dreyer, G. F. (1975): "Effects of Temperature and Humidity Fluctuations on the Optical Refractive Index in the Marine Boundary Layer." J. Opt. Soc. Amer., 65, 1502-1511.

Friehe, C. A. and Schmitt, K. F., (1976): "Parameterization of Air-Sea Interface Fluxes of Sensible Heat and Moisture by the Bulk Aerodynamic Formulas," J. Phys. Oceanogr., 6, 801-809.

Houlihan, T. M., Davidson, K. L., Fairall, C. W., and Schacher, G. E., (1978): "Experimental Aspects of a Shipboard System Used in Investigation of Overwater Turbulence and Profile Relationships," I.E.E.E., J. of Oceanogr. Instr. (submitted).

Kondo, J. (1975): "Air-Sea Bulk Transfer Coefficients in Diabatic Conditions," Boundary Layer Meteorology, 9, 91-112.

Liu, W. T. (1978): "The Molecular Effects on Air-Sea Exchanges," Ph.D. Dissertation, University of Washington, Seattle, WA, 170 pp.

Muller-Glewe, J. and Hinzpeter, H., (1974): "Measurement of the Turbulent Heat Flux Over the Sea," Boundary Layer Meteorol., 6, 47-52.

Plunkett, J. R. (1976): "A Microprogrammable Data Acquisition and Control System (MIDAS II A) with Application to Mean Meteorological data," M. S. Thesis, Naval Postgraduate School, Monterey, CA 144 pp.

Pond, S., Fissel, D. B., and Paulson, C. A. (1974): "A Note on Bulk Aerodynamic Coefficients for Sensible Heat and Moisture Fluxes," Boundary Layer Meteorol., 6, 333-340.

Schmitt, K. F., Friehe, C. A., and Gibson C. H. (1978): "Humidity Sensitivity of Atmospheric Temperature Sensors by Salt Contamination," J. Phys. Oceanogr., 8, 115-161.

Smith, S. D., (1974): "Eddy Flux Measurements over Lake Ontario," Boundary Layer Meteor., 6, 235-256.

Wyngaard, J. C. (1973): "On Surface-Layer Turbulence," Chapter 3, Workshop on Micrometeorology, D. Haugen, Editor, American Meteorological Society, 101-149.

Wyngaard, J. C., Izumi, Y., and Collins, S. A., (1971): "Behavior of the Refractive Index Structure Parameter near the Ground," J. Opt. Soc. Am., 61, 1646-1650.

LIST OF TABLES

Table 1. C_{DN} versus wind speed (10 meter) from Kondo (1975).

$U\ ms^{-1}$	$C_{DN} \times 10^3$
.3 - 2.2	$1.08 \times U^{-.15}$
2.2 - 5.0	$.77 + .086 \times U$
5.0 - 8.0	$.87 + .067 \times U$
8.0 - 25.0	$1.2 + .025 \times U$

TABLE 2. Summary of Experiments

EXPERIMENT	SHIP	LOCATION	PERIOD	NUMBER OF PERIODS
	R/V ACANIA[4]	Monterey Bay	All Months 1973-76	98
CEWCOM-76[1]	R/V ACANIA	E. Pacific	Sep-Oct 76	285
NRL - EOMET[2]	USNS HAYES[5]	N. Atlantic & Mediterranean	May-Jun 77	269
	USNS KANE[6]	Mid-Atlantic	Feb-Mar 78	38
CEWCOM-78[3]	R/V ACANIA	E. Pacific	May 1978	200
			Total	890

[1]Cooperative Experiment West Coast Oceanography & Meteorology-1976

[2]Naval Research Laboratories, Electro-Optical Meteorology Cruise

[3]Cooperative Experiment West Coast Oceanography & Meteorology-1978

[4]Operated by Department of Oceanography, Naval Postgraduate School, Monterey, California

[5]Operated by Naval Research Laboratories, Washington, D. C.

[6]Operated by Naval Oceanographic Office, Washington, D. C.

Table 3. Error analysis for measured, intermediate, and scaling parameters

Measured	T_S	T_Z	U	RH	C_T^2
RMS Error (±)	.3°C	.2°C	8%	3%	30%

Intermediate	Δθ	ΔQ
Accuracy (±)	.5°C	.4 gm/Kg

Scaling	U_*	T_*	Q_*	ξ
Accuracy (±)	10%	.02°C	.02 gm/Kg	.03 or 30%

Table 4. Empirically determined sensible heat drag coefficients, x 10^3

Sources	C_{HN}	C_{DN}	$C_{\theta N}$
Pond, et al. (1974)	1.5	1.45	1.55
Dunckel, et al. (1974)	1.5	1.60	1.40
Muller-Glewe and Hinzpeter (1974)	1.0	(1.30)[1]	.77
Smith (1974)	1.2	1.02	1.41
Friehe and Schmitt (1976)	.91[2]	(1.30)	.64
This study	1.3	1.30	1.34

[1]( ) denotes assumed C_N value; other given by authors

[2]Excludes high wind data

Figure 1. Ratio of ξ based on stability dependent drag coefficients (ξ) to ξ based on constant drag coefficients (ξ_o) versus ξ_o.

Figure 2. Schematics of shipboard mounting arrangements, (a) R/V ACANIA, (b) USNS HAYES, and (c) USNS KANE.

Figure 3. Ratio of C_T^2 (before to after replacement or washing) versus RH; (From CEWCOM-78).

Figure 4. Ratio of measured C_T^2 to computed C_T^2 (from Eq. 5) versus RH, for all except CEWCOM-78 data.

Figure 5. C_T^2 versus $\Delta\theta$ (a) daytime (0800-1900 LST), (b) nightime (1900-0800 LST).

Figure 6. Mean DTSP versus ξ results. Solid curve is prediction based on Eq. 5.

Figure 7. $C_{\theta N}$ versus ξ results. $C_{\theta N}$ based on Eq. 17 and CEWCOM-78 results.

Figure 8. Same as Figure 6 with logarithmic ξ axis.

Figure 9. DTSP based on asymptotic scaling (a) free convection curve is approximate prediction, Eq. 18 and, (b) Z-less, curve is prediction, Eq. 19.

Figure 10. Height variations of C_T^2 versus ξ. $A(C_T^2)$ is defined by Eq. 20, solid curves are prediction based on Eq. 5.

Figure 11. Results from 24 hour period during CEWCOM-78 (a) Observed and Predicted C_T^2 for 10 meters (b) Observed ξ.

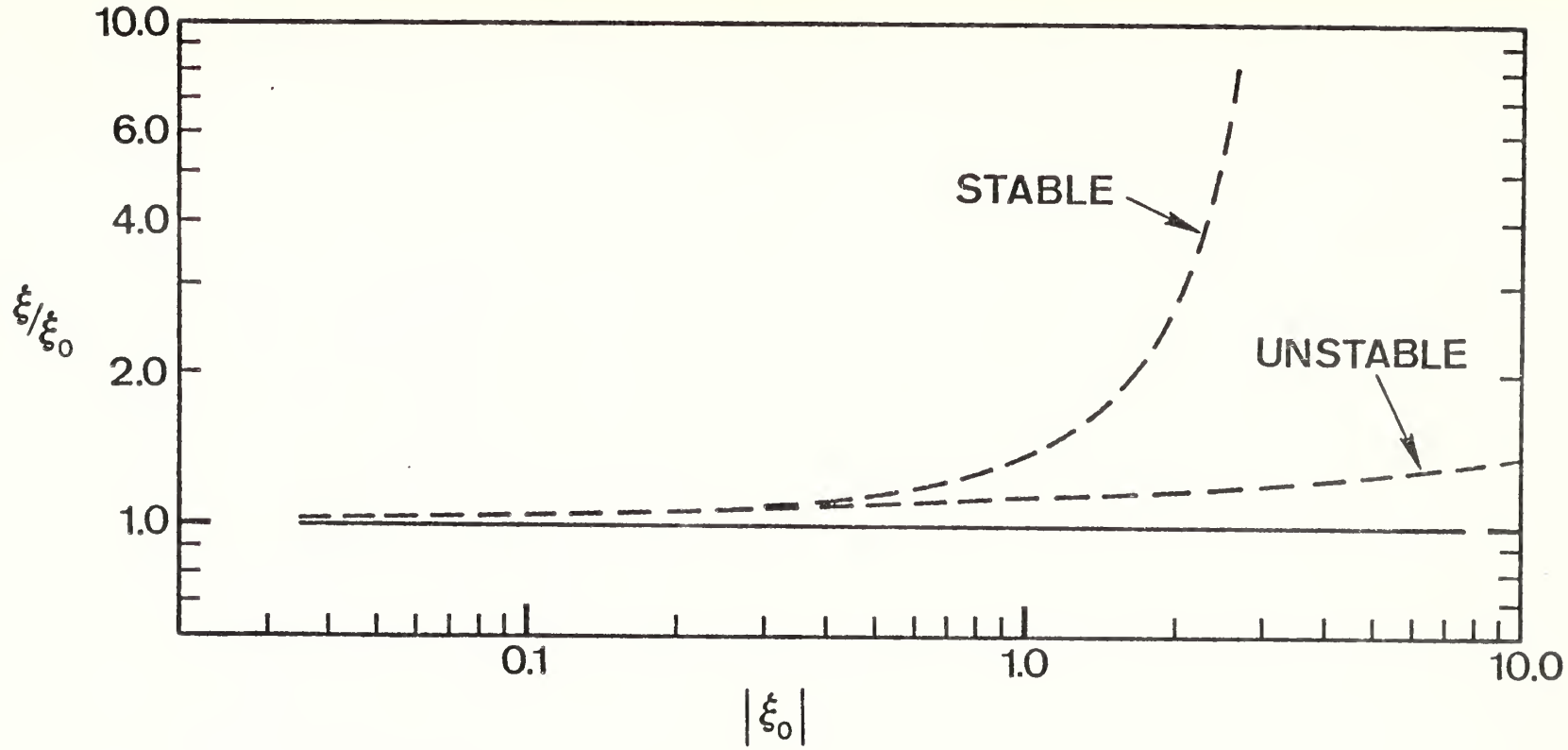

Figure 1. Ratio of ξ based on stability dependent drag coefficients (ξ) to ξ based on constant drag coefficients (ξ_o) versus ξ_o.

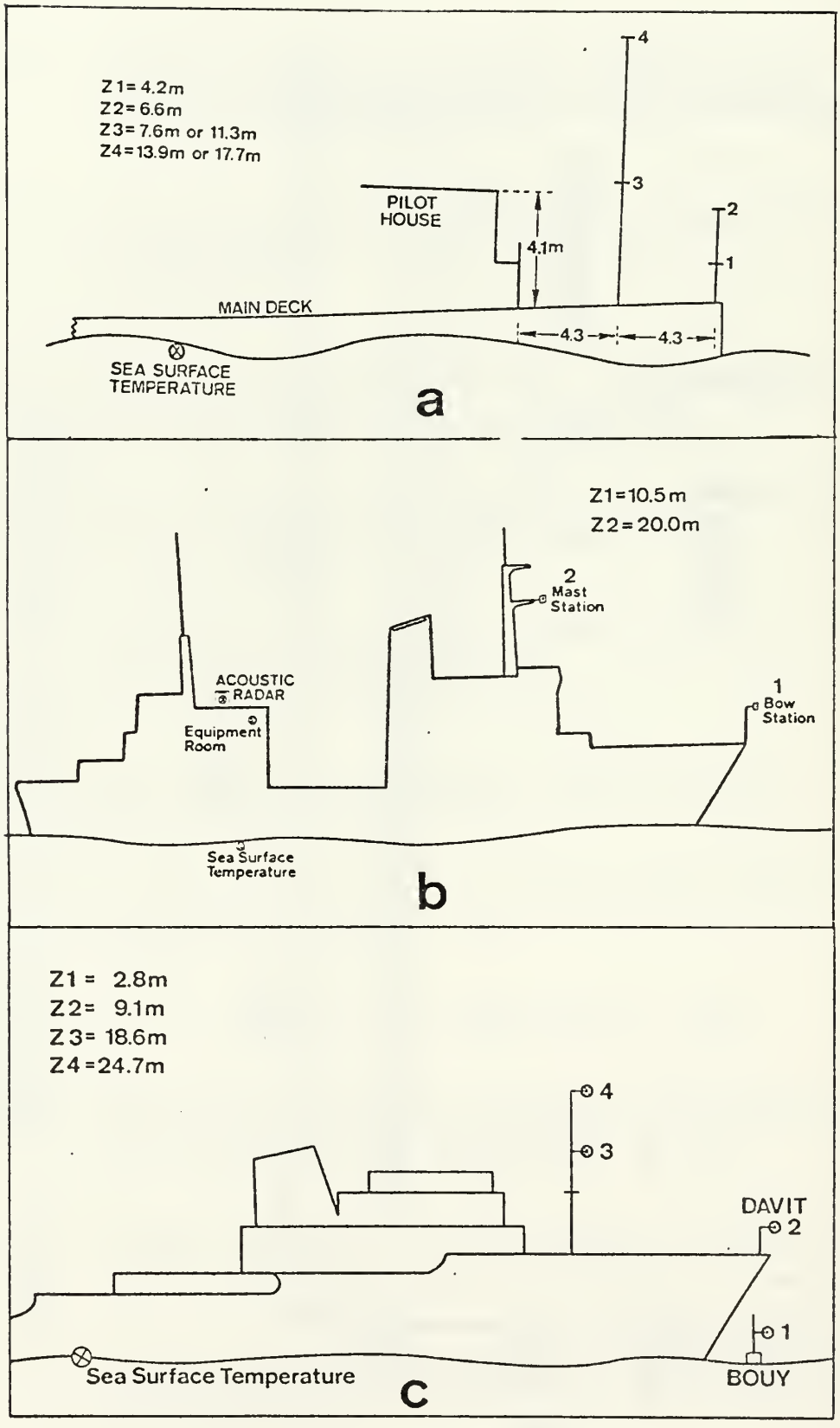

Figure 2. Schematics of shipboard mounting arrangements, (a) R/V ACANIA, (b) USNS HAYES, and (c) USNS KANE.

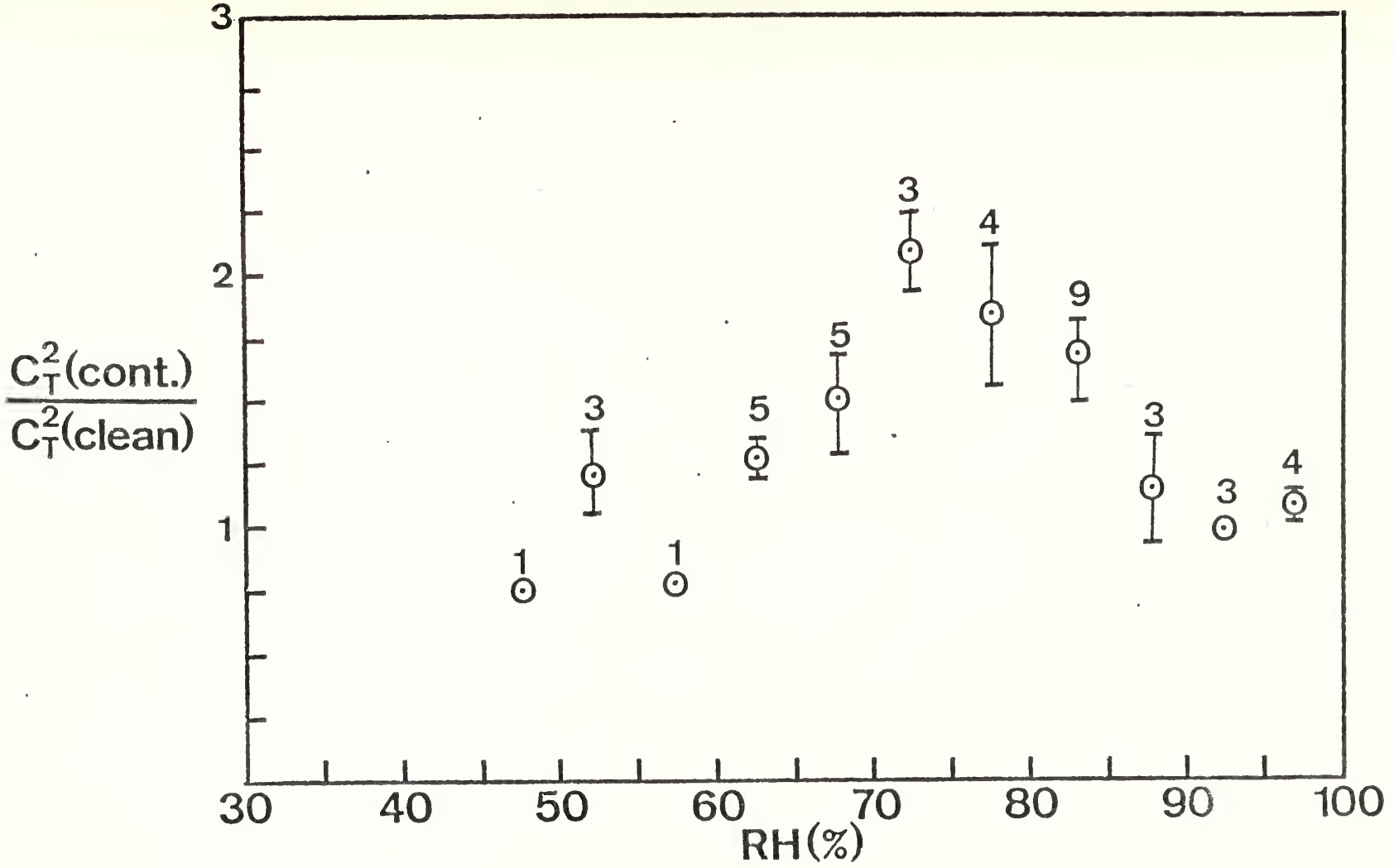

Figure 3. Ratio of C_T^2 (before to after replacement or washing) versus RH; (From CEWCOM-78).

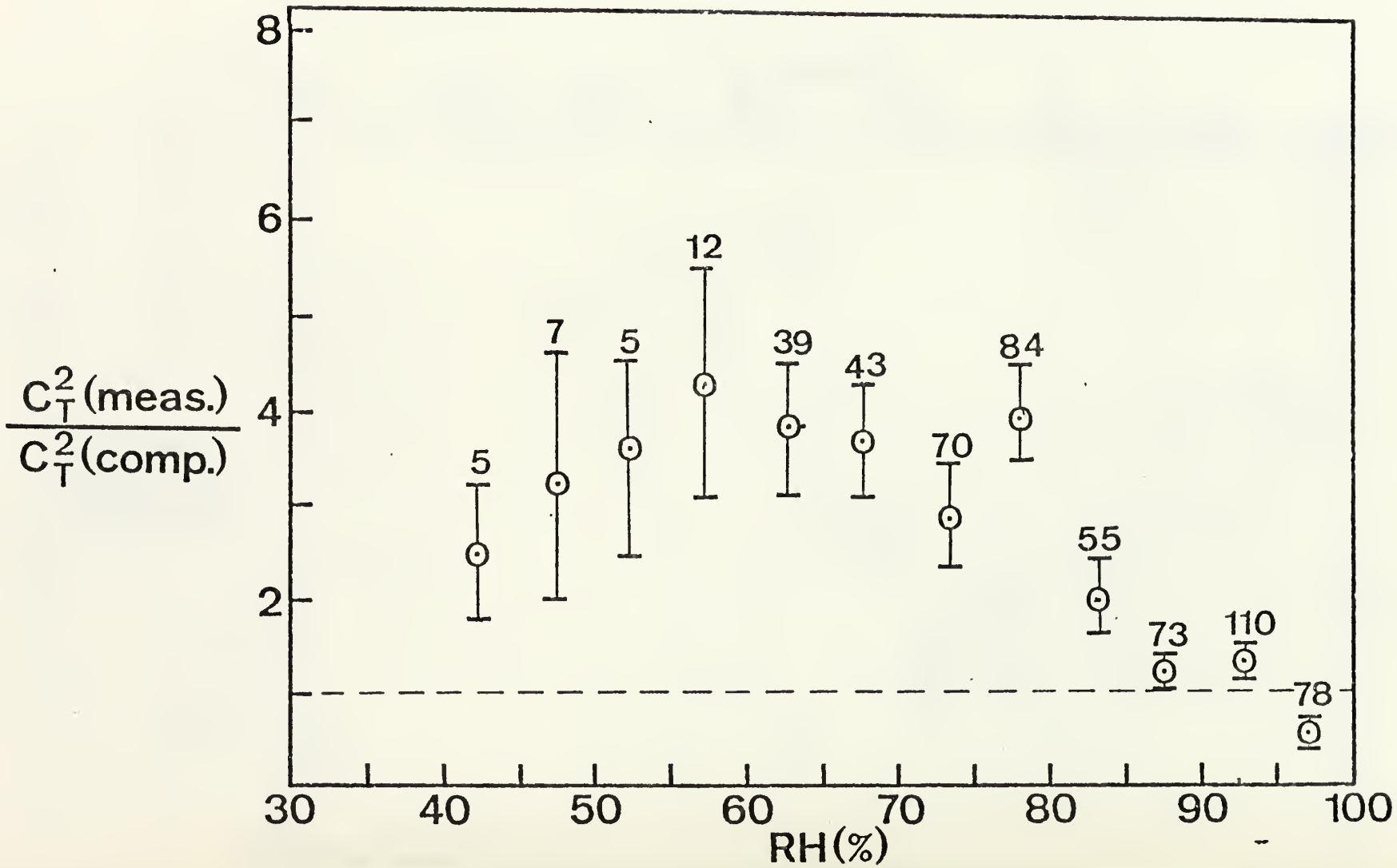

Figure 4. Ratio of measured C_T^2 to computed C_T^2 (from Eq. 5)

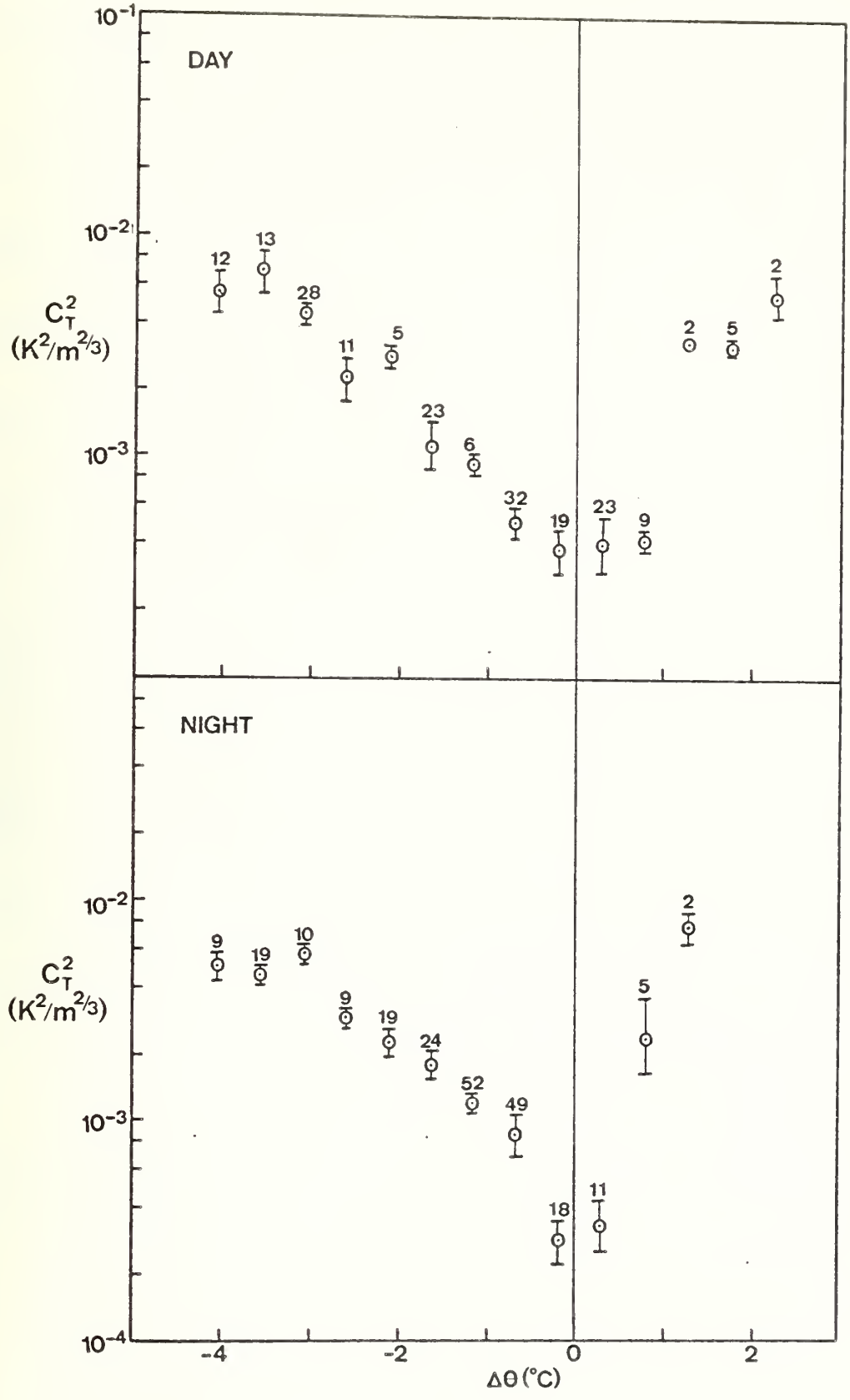

Figure 5. C_T^2 versus $\Delta\theta$ (a) daytime (0800-1900 LST), (b) nightime (1900-0800 LST).

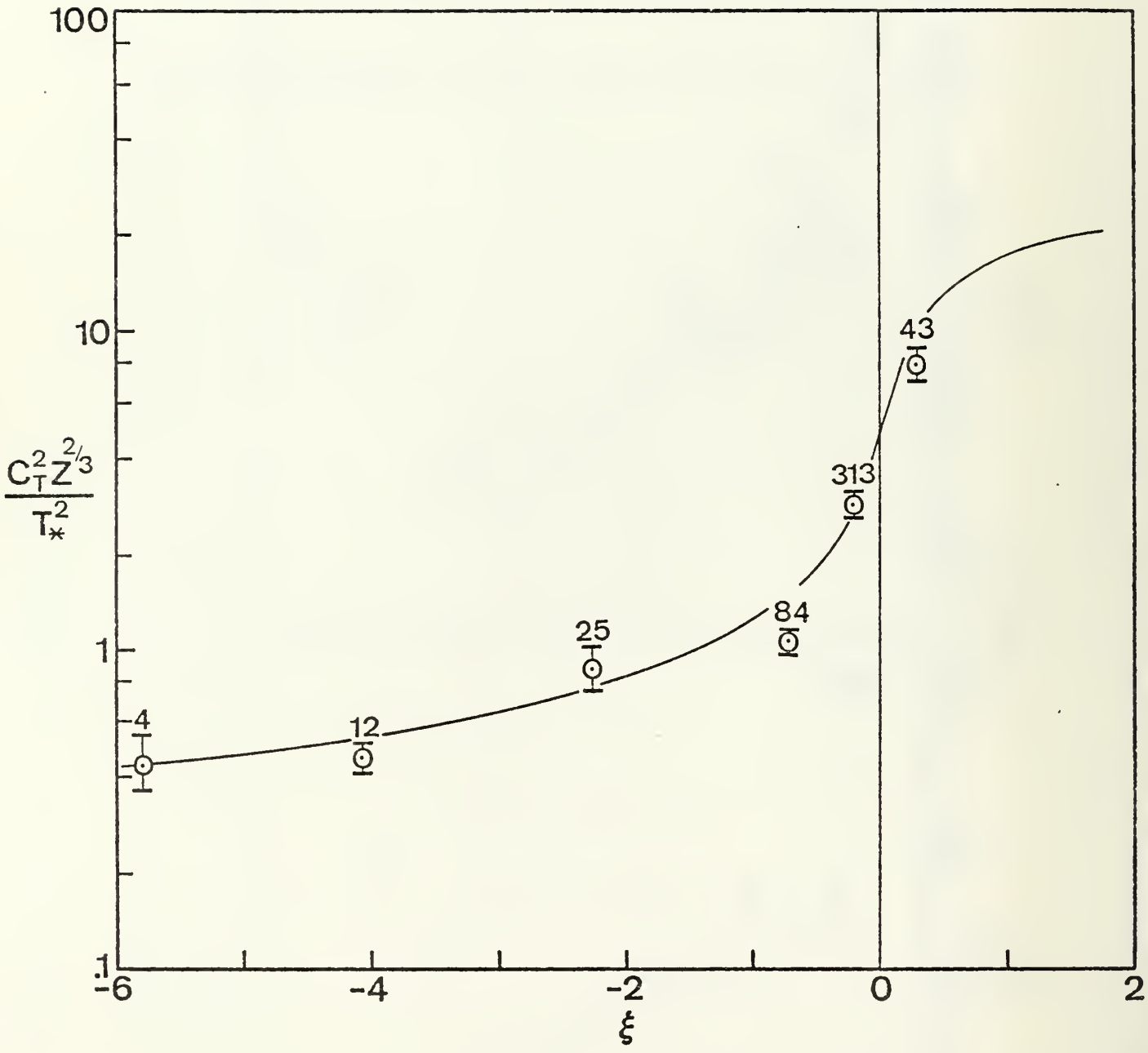

Figure 6. Mean DTSP versus ξ results. Solid curve is prediction based on Eq. 5.

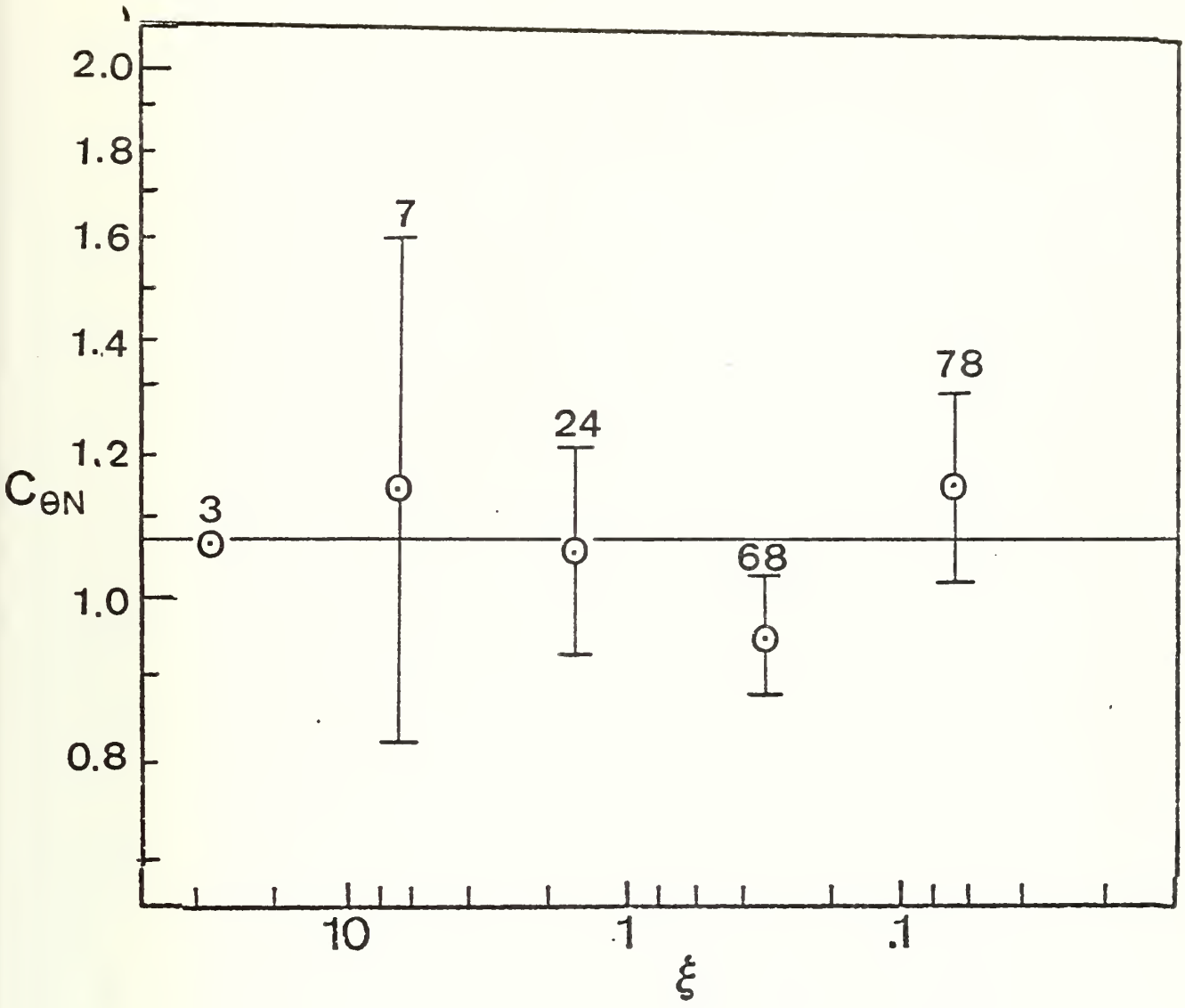

Figure 7. $C_{\theta N}$ versus ξ results. $C_{\theta N}$ based on Eq. 17 and CEWCOM-78 results.

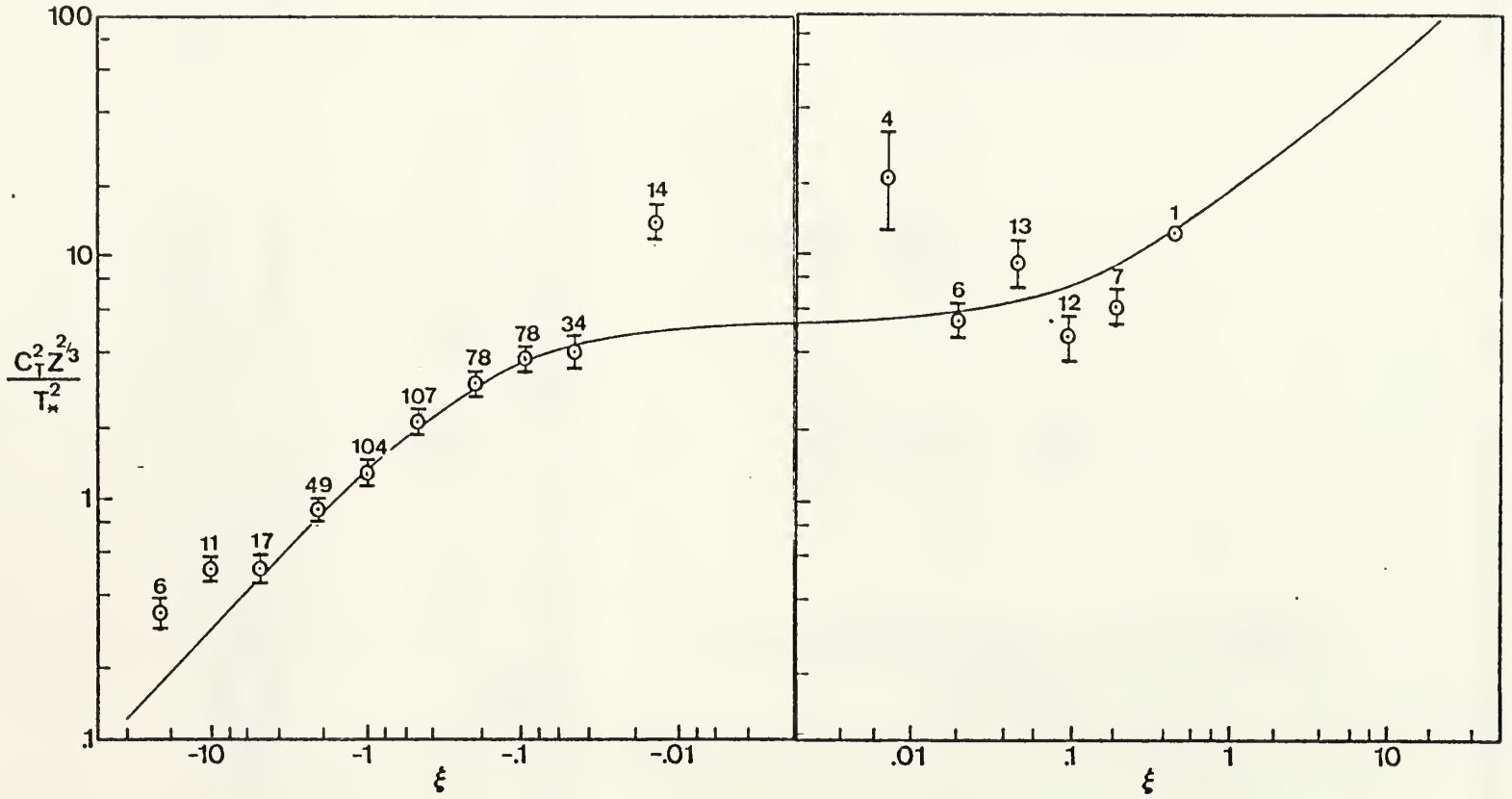

Figure 8. Same as Figure 6 with logarithmic ξ axis.

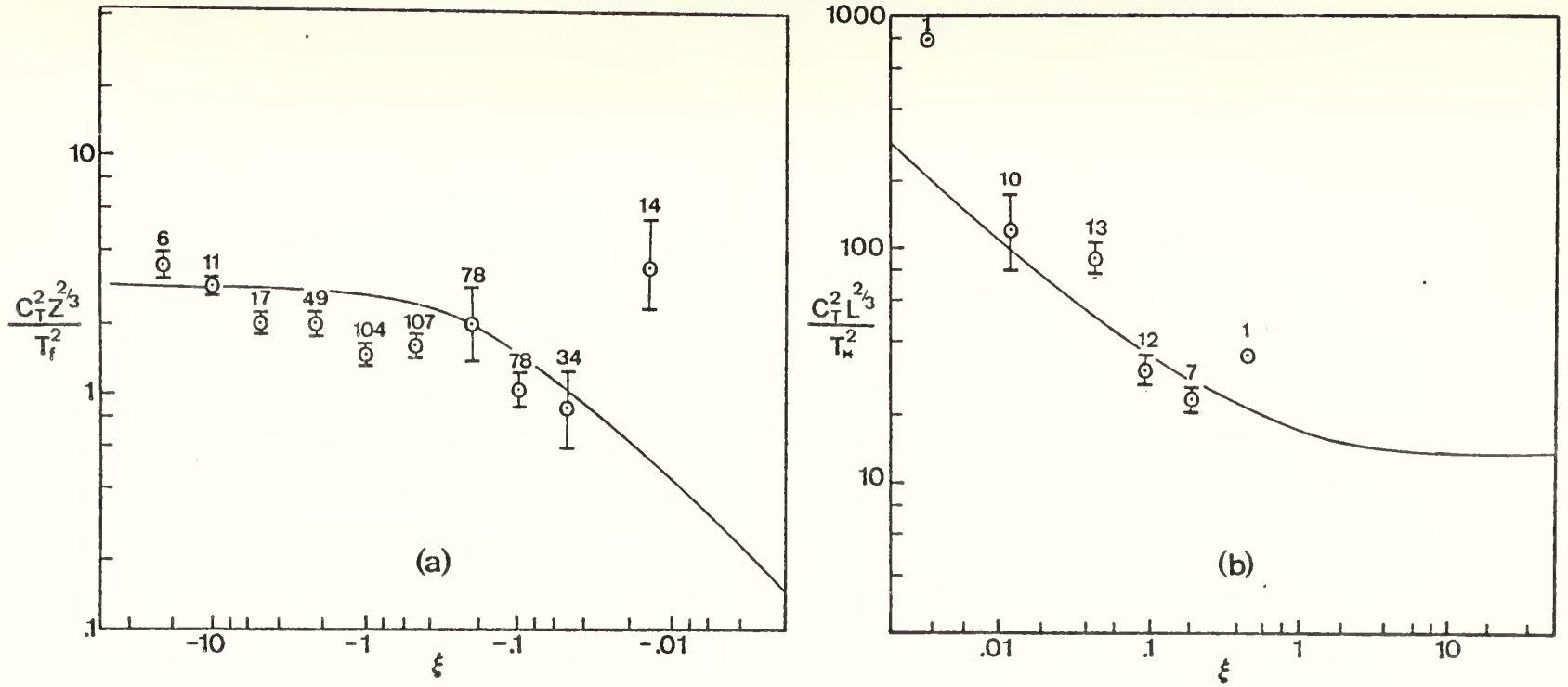

Figure 9. DTSP based on asymptotic scaling (a) free convection curve is approximate prediction, Eq. 18 and, (b) Z-less, curve is prediction, Eq. 19.

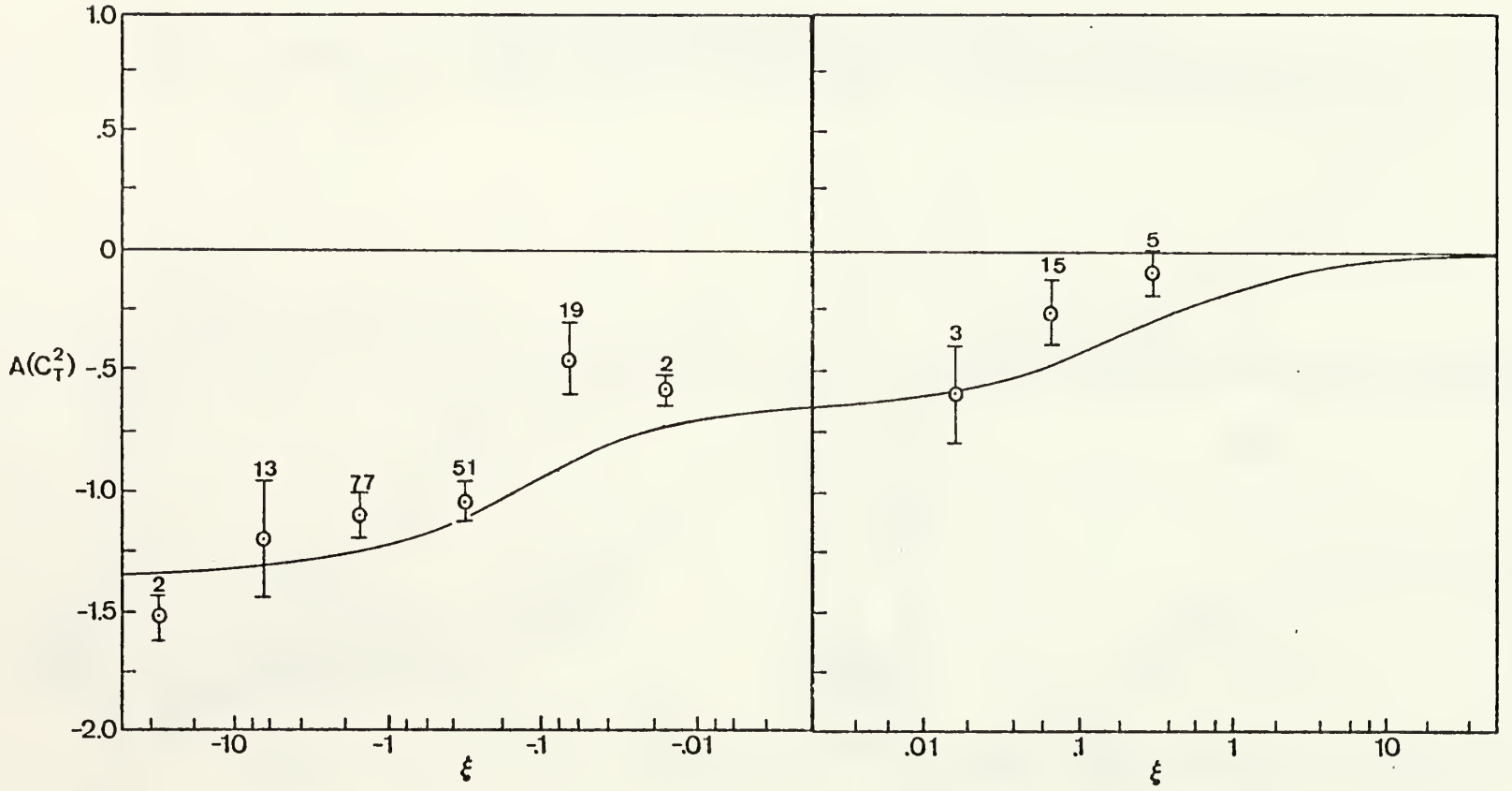

Figure 10. Height variations of C_T^2 versus ξ. $A(C_T^2)$ is defined by Eq. 20, solid curves are prediction based on Eq. 5.

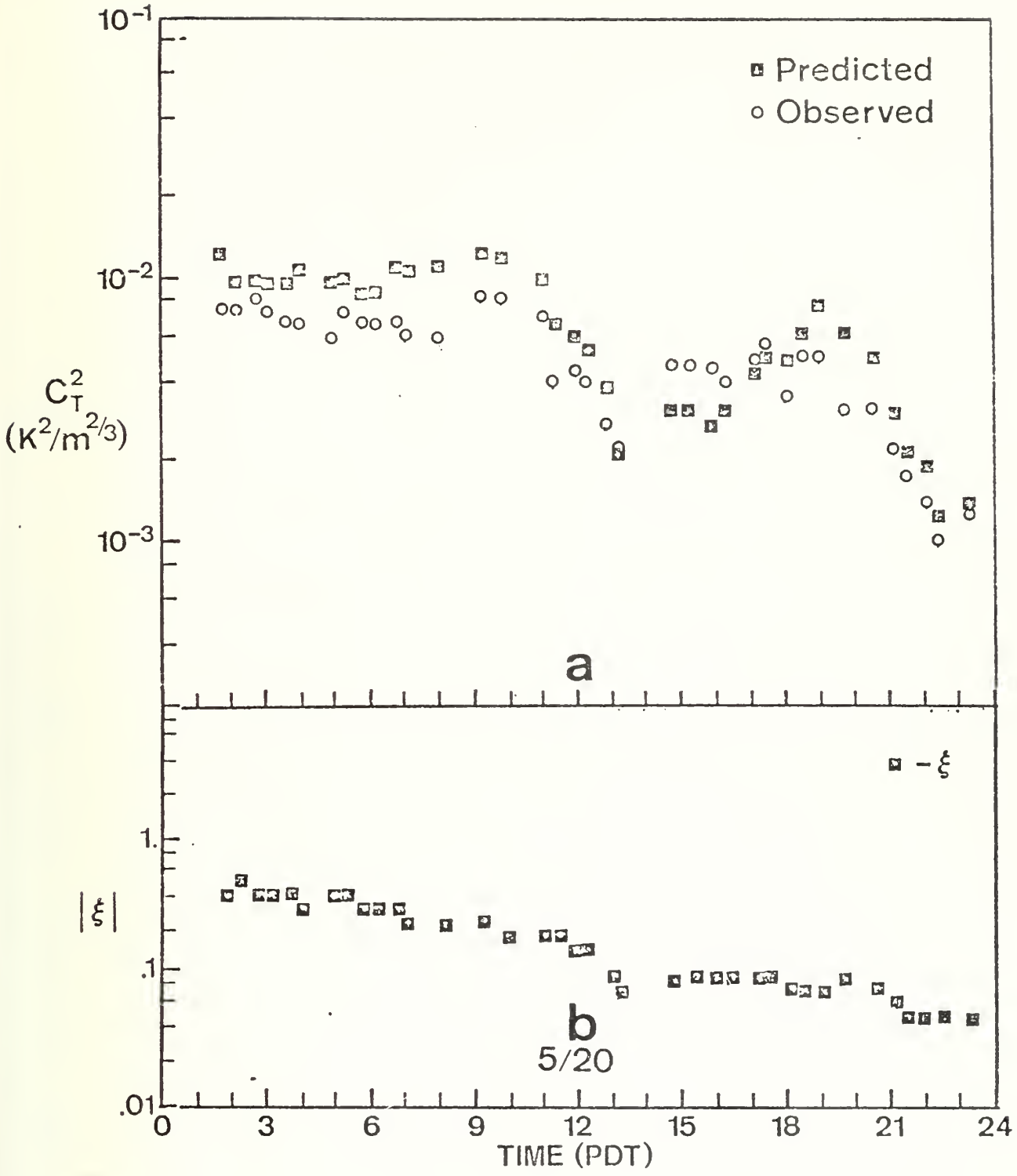

Figure 11. Results from 24 hour period during CEWCOM-78
(a) Observed and Predicted C_T^2 for 10 meters
(b) Observed ξ.

INITIAL DISTRIBUTION LIST

		No. of Copies
1.	Defense Documentation Center Cameron Station Alexandria, Virginia 22314	2
2.	Library, Code 0212 Naval Postgraduate School Monterey, California 93940	2
3.	Dean of Research, Code 012 Naval Postgraduate School Monterey, California 93940	1
4.	Asst. Professor C. W. Fairall, Code 61Fr Naval Postgraduate School Monterey, California 93940	5
5.	Professor K. E. Woehler, Code 61Wh Naval Postgraduate School Monterey, California 93940	1
6.	Dr. Ralph Markson Airborne Research Associates 46 Kendal Common Road Weston, Massachusetts 02193	1
7.	Assoc. Professor K. L. Davidson, Code 63Ds Naval Postgraduate School Monterey, California 93940	5
8.	Assoc. Professor T. Houlihan, Code 69Hm Naval Postgraduate School Monterey, California 93940	5
9.	Assoc. Professor G. Schacher, Code 61Sq Naval Postgraduate School Monterey, California 93940	5
10.	Mr. Murray Schefer Code Air-3706 Naval Air Systems Command Washington, D. C. 20360	1
11.	LT Michelle Hughes PM-22/PMS 405 Naval Sea Systems Command Washington, D. C. 20362	1

No. of Copies

12. Dr. Stuart Gathman
Code 8326
Naval Research Laboratory
Washington, D. C. 20375 1

13. Dr. Lothar Rohnke
Code 8320
Naval Research Laboratory
Washington, D. C. 20375 1

14. Dr. Barry Katz
Code 231
Naval Surface Weapons Center
White Oak Laboratory
Silver Spring, Maryland 20910 1

15. Professor Dale Leipper, Code 68Lr
Naval Postgraduate School
Monterey, California 93940

16. Eugene J. Mack
Calspan Corporation
Buffalo, New York 14221 1

17. Theodore V. Blanc
Code 8322B
Naval Research Laboratory
Washington, D. C. 20375 1

18. Dr. J. H. Richter
Code 813
Submarine Systems Division
Communications Systems and Technology Department
Naval Oceans Systems Center
San Diego, California 92152 1